JCB Journal of Cell Biology

REPORT

Oligomerization of the FERM-FA protein Yurt controls epithelial cell polarity

Clémence L. Gamblin, Frédérique Parent-Prévost, Kévin Jacquet, Cornélia Biehler, Alexandra Jetté, and Patrick Laprise

Drosophila melanogaster **Yurt (Yrt) and its mammalian orthologue EPB41L5 limit apical membrane growth in polarized epithelia. EPB41L5 also supports epithelial–mesenchymal transition and metastasis. Yrt and EPB41L5 contain a four-point-one, ezrin, radixin, and moesin (FERM) domain and a FERM-adjacent (FA) domain. The former contributes to the quaternary structure of 50 human proteins, whereas the latter defines a subfamily of 14 human FERM proteins and fulfills unknown roles. In this study, we show that both Yrt and EPB41L5 oligomerize. Our data also establish that the FERM-FA unit forms an oligomeric interface and that multimerization of Yrt is crucial for its function in epithelial cell polarity regulation. Finally, we demonstrate that aPKC destabilizes the Yrt oligomer to repress its functions, thereby revealing a mechanism through which this kinase supports apical domain formation. Overall, our study highlights a conserved biochemical property of fly and human Yrt proteins, describes a novel function of the FA domain, and further characterizes the molecular mechanisms sustaining epithelial cell polarity.**

Introduction

Epithelial cell polarity is established and maintained by local positive feedback loops and through mutual antagonism opposing lateral and apical protein modules (Tepass, 2012). For instance, the lateral polarity protein Yurt (Yrt) limits the activity of the apical kinase atypical PKC (aPKC), which represses Yrt functions (Gamblin et al., 2014). This reciprocal functional relationship contributes to establishing a precise demarcation between the apical and lateral domains. Yrt encloses a four-point-one, ezrin, radixin, and moesin (FERM) domain at its N terminus (Tepass, 2009; Baines et al., 2014). The FERM domain is a three-lobed structure that sustains protein–protein and protein–lipid interactions. The N-terminal F1 lobe, the central F2 lobe, and the C-terminal F3 lobe fold independently but associate closely to form a cloverleaf-like structure (Hamada et al., 2000; Pearson et al., 2000). Yrt also contains a FERM-adjacent (FA) domain that defines a subgroup of FERM family members (Baines, 2006; Tepass, 2009). The FA domain is ∼60 amino acids long and forms a putative folded structure contiguous to the C-terminal end of the FERM domain (Baines, 2006; Baines et al., 2014). Mammals express two Yrt orthologues, namely erythrocyte membrane protein band 4.1 like 5 (EPB41L5; also known as Lulu and YMO1) and expressed in highly metastatic cells 2 (EHM2; also referred to as Lulu2 and EPB41L4B; Tepass, 2009). Fly and vertebrate Yrt proteins share an evolutionarily conserved function in stabilizing the lateral membrane and restricting apical membrane growth (Hsu et al., 2006; Laprise et al., 2006, 2009; Gosens et al., 2007).

aPKC phosphorylates the FA domain of Yrt, thereby favoring the apical exclusion of Yrt in immature epithelial cells (Gamblin et al., 2014). This phosphorylation represses Yrt function and is critical to preserve the integrity of the apical membrane and to establish the functional architecture of epithelial tissues. Hence, elucidating how aPKC phosphorylation impacts the activity of Yrt proteins currently remains a puzzle, the solving of which will help delineate the molecular mechanisms regulating epithelial cell polarity, epithelial–mesenchymal transition (EMT), and cancer biology. We hypothesized that the phosphorylation of Yrt by aPKC could alter protein–protein interactions important for Yrt activity including possible homo-oligomerization.

Results and discussion

Yrt and its mammalian orthologue EPB41L5 oligomerize

To investigate whether Yrt forms an oligomer, we first established a transgenic fly line coexpressing HA-tagged and FLAG-tagged Yrt proteins. Transgenic animals coexpressing FLAG-Yrt together with HA-RFP or FLAG-GFP with HA-Yrt were used as negative controls. Coimmunoprecipitation experiments revealed that HA-Yrt and FLAG-Yrt are part of a common mac-

Centre de Recherche sur le Cancer de l'Université Laval, and Axe Oncologie du Centre de Recherche du Centre Hospitalier Universitaire de Québec-Université Laval, Québec City, Canada.

Correspondence to Patrick Laprise: Patrick.Laprise@crchudequebec.ulaval.ca.

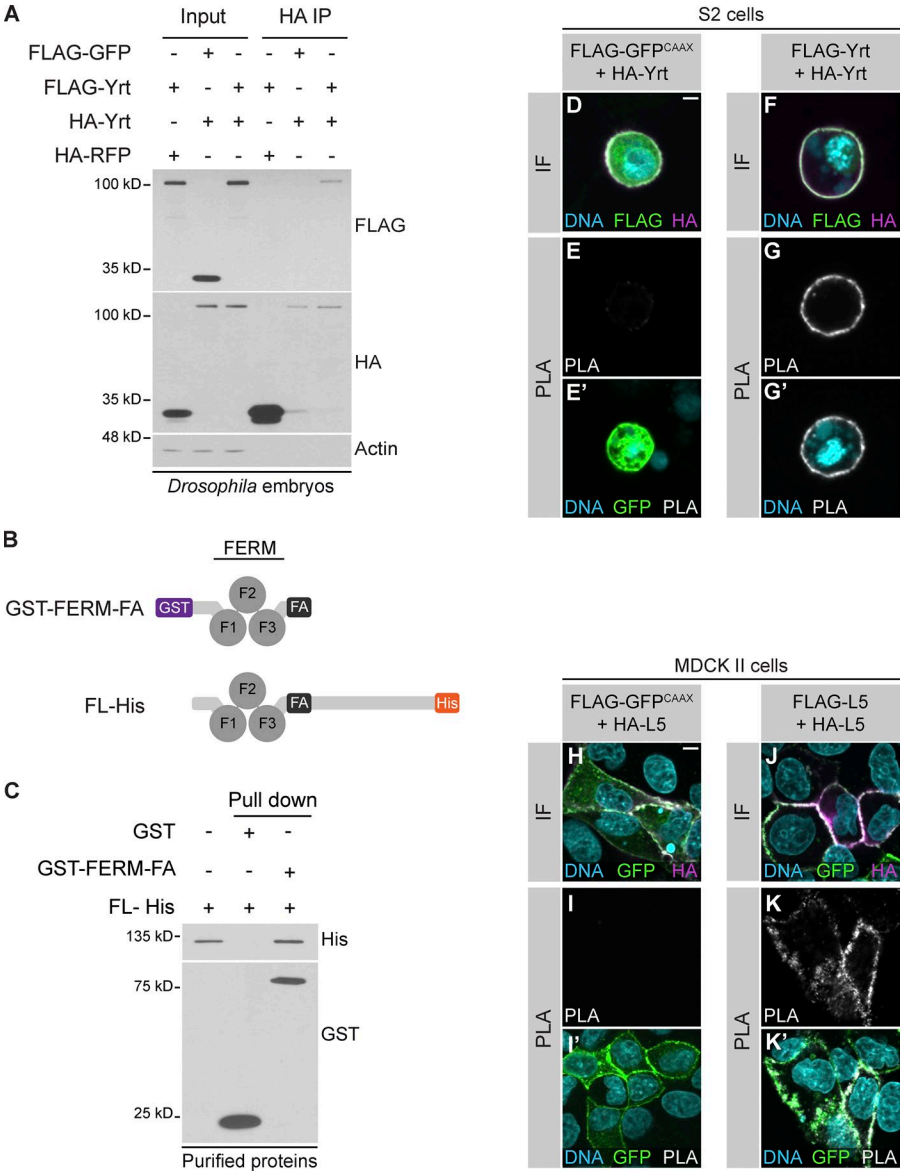

Figure 1. **Yrt and EPB41L5 oligomerize. (A)** Stage 15–17 *Drosophila* embryos expressing FLAG-Yrt with HA-RFP, FLAG-GFP with HA-Yrt, or FLAG-Yrt with HA-Yrt were homogenized. An immunoprecipitation with anti-HA antibodies was then performed (HA IP), and eluted proteins were detected by Western blotting. A portion of each homogenate was retained to monitor protein expression. **(B)** Schematics of the fusion proteins used to investigate whether the Yrt–Yrt interaction is direct. **(C)** Purified FL-His was mixed with either GST or GST–FERM-FA, and a GST pulldown was performed. Pulled-down proteins were detected by Western blotting. **(D–G)** S2 cells were cotransfected with FLAG-GFP^{CAAX} and HA-Yrt (D and E) or with FLAG-Yrt and HA-Yrt (F and G). Cells were then processed for immunofluorescence (IF) with anti-FLAG and anti-HA antibodies (D and F) or for PLA (E and G). Intrinsic GFP fluorescence was used to detect transfected cells in E. DNA was stained by using DAPI. **(H–K)** MDCK II cells coexpressing FLAG-GFP^{CAAX} with HA-EPB41L5 (HA-L5) or GFP-EPB41L5 (GFP-L5) with HA-L5 were fixed and costained for GFP and HA (H and J) or submitted to a PLA (I and K). GFP fluorescence was used to detect transfected cells in I and K. Bars, 5 µm.

romolecular complex in *Drosophila melanogaster* embryos (Fig. 1 A). Similarly, a purified GST-tagged truncated Yrt protein containing the FERM and FA domains efficiently pulled down purified, full-length Yrt in fusion with a His tag (Fig. 1, B and C). This demonstrates that parts of the FERM-FA unit contribute to the Yrt–Yrt interaction, which is direct. To further support this latter conclusion, we used an in situ proximity ligation assay (PLA) that detects direct protein–protein interactions in intact cells (Söderberg et al., 2006). Although FLAG-GFP^{CAAX} and HA-Yrt colocalized but displayed minimal PLA staining (Fig. 1, D and E), complete colocalization and a strong PLA signal were observed at the membrane of S2 cells coexpressing FLAG-Yrt and HA-Yrt (Fig. 1, F and G). This shows that Yrt self-associates in cellulo. Similarly, clear colocalization and a positive PLA staining were observed at cell–cell contacts in MDCK II cells coexpressing HA-tagged EPB41L5 and GFP-EPB41L5 (Fig. 1, J and K). The absence of a PLA signal in MDCK II cells expressing FLAG-GFP^{CAAX} and HA-EPB41L5 confirmed the specificity of the interaction (Fig. 1, H and I). Altogether, these data show that Yrt and EPB41L5 share an evolutionarily conserved ability to oligomerize.

The FERM and FA domains form an oligomeric interface

Our pulldown experiment showed that the N-terminal half of Yrt contributes to self-association of this protein (Fig. 1 C). To further define the domain(s) sustaining Yrt oligomerization, we generated and coexpressed FLAG-tagged Yrt truncations (Fig. 2 A) with full-length HA-tagged Yrt in S2 cells. Then, we performed an immunoprecipitation using anti-HA antibodies. As expected, full-length FLAG-Yrt formed a complex with HA-Yrt (Fig. 2 B). Likewise, the truncation containing the FERM and FA domains showed a strong association with HA-Yrt (Fig. 2 B). In contrast, the FERM domain alone exhibited a very weak ability to bind to HA-Yrt, whereas the truncation extending from the FA domain to the C terminus or the construct covering only the C-terminal portion of Yrt was not coimmunoprecipitated with HA-Yrt (Fig. 2 B). These results suggest that the FERM and FA domains are both required for optimal oligomerization of Yrt. Accordingly, removal

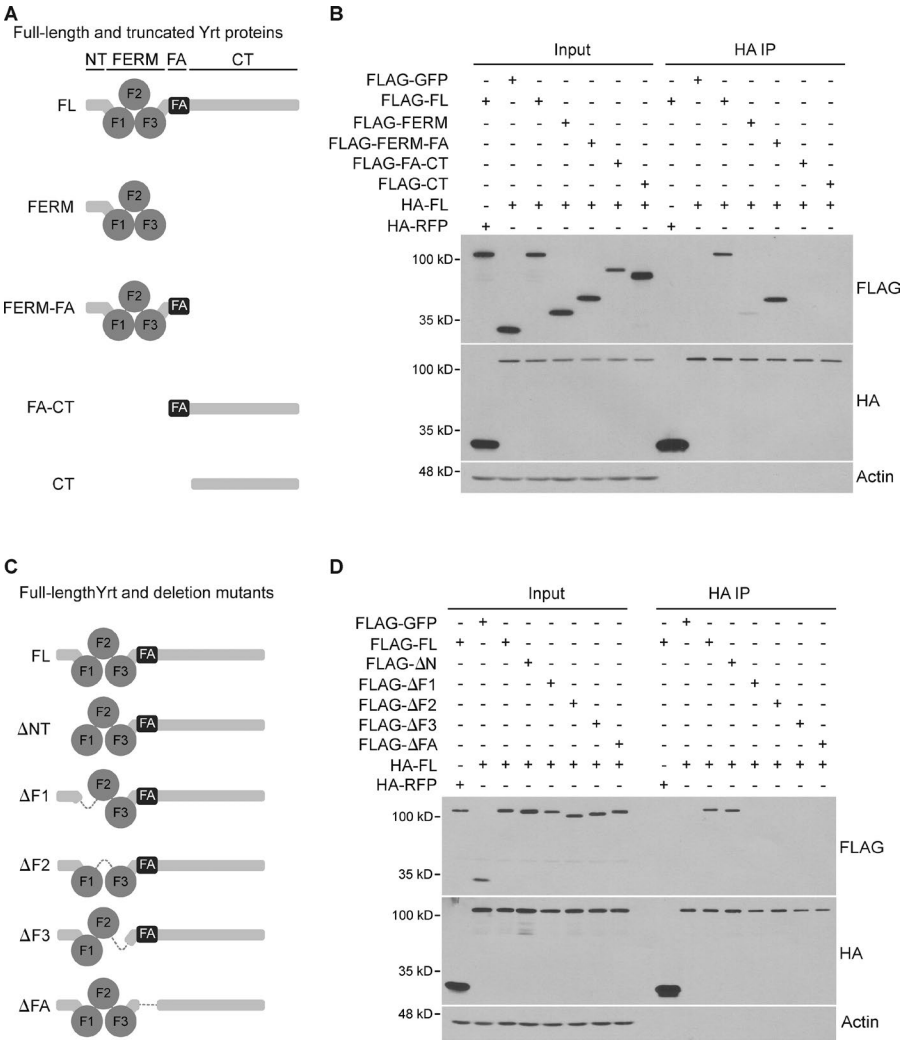

Figure 2. **The oligomerization of Yrt requires the FERM and FA domains. (A and C)** Schematics of the Yrt proteins used in B and D, respectively. HA or FLAG tags were added to the N terminus of the following proteins: full-length (FL; aa 1–972), FERM (aa 1–349), FERM-FA (aa 1–415), FA-CT (aa 330–972), CT (aa 406–972), ΔN-Terminal (ΔNT; aa 57–972), ΔF1 (aa 1–56/139-972), ΔF2 (aa 1–141/254-972), ΔF3 (aa 1–253/346-972), and ΔFA (aa 1–351/394-972). FLAG-GFP and HA-RFP were used as controls. **(B and D)** S2 cells were transfected with the indicated constructs and homogenized. HA-Yrt or HA-RFP was then immunoprecipitated, and Western blotting was used to investigate the presence of tagged proteins in protein complexes.

of any lobe of the FERM domain or deletion of the FA domain totally disrupted Yrt self-association, whereas deletion of the portion of Yrt N-terminal to the FERM domain had no impact (Fig. 2, C and D). Similar to WT Yrt, most modified proteins showing impaired oligomerization localized to the membrane (Fig. S1), demonstrating that the lack of coimmunoprecipitation of these FLAG-tagged proteins with HA-Yrt does not result from altered subcellular localization. Together, these results demonstrate that the FERM-FA unit of Yrt defines an oligomerization interface.

Oligomerization of Yrt is essential for its function in epithelial cell polarity

To investigate the functional relevance of Yrt oligomerization, we aimed to produce point mutations interfering with Yrt self-association. The Yrt–Yrt association resists in a high salt concentration, thus suggesting that it is based on hydrophobic interactions (not depicted). Interestingly, the F3 lobe of the FERM domain of all fly FERM-FA proteins (Yrt, Cora, Cdep, Ptpmeg, CG5022, and CG34347; Tepass, 2009), human EPB41L5, and human EHM2 contains well-conserved hydrophobic amino acids (Fig. 3 A). Knowing that the F3 lobe is required for Yrt oligomerization (Fig. 2 D), we mutagenized these hydrophobic residues in pairs (phenylalanine [F] 281 with tryptophan [W] 283, and F316 with W328; Fig. 3 A) and investigated the impact of these mutations on Yrt oligomerization in S2 cells. F281 and W283 were mutagenized to neutral alanine (A), negatively charged aspartate (D), or positively charged arginine (R), whereas F316 and W328 were replaced by A residues. Although FLAG-Yrt^{F316A,W328A} displayed a reduced interaction with HA-Yrt compared with WT FLAG-Yrt (Fig. 3 B), mutation of F281 and W283 to A, D, or R almost completely abolished Yrt oligomerization as shown by coimmunoprecipitation experiments (Fig. 3 B). A PLA confirmed the lack of oligomerization of the FLAG-Yrt^{F281R,W283R} mutant protein, which localized to the membrane (Fig. 3, C and D). This shows that we have successfully targeted residues required for Yrt oligomerization. Moreover, this indicates that within the F3 lobe of the FERM domain, F281 and W283 are particularly important for Yrt self-association. Based on these results, we used CRISPR/Cas9-mediated genome editing to produce a fly line expressing Yrt^{F281R,W283R} from the endogenous *yrt* locus. To explore the impact of this mutation on protein expression and localization, we isolated embryos devoid of maternal Yrt, which were obtained from germ line clone females (null allele *yrt*^{75}; Chou and Perrimon, 1996; Laprise et al., 2006), and carrying the *yrt*^{F281R,W283R} allele. Embryos lacking maternal Yrt but having a WT paternal copy of *yrt* (+) were used as a positive control

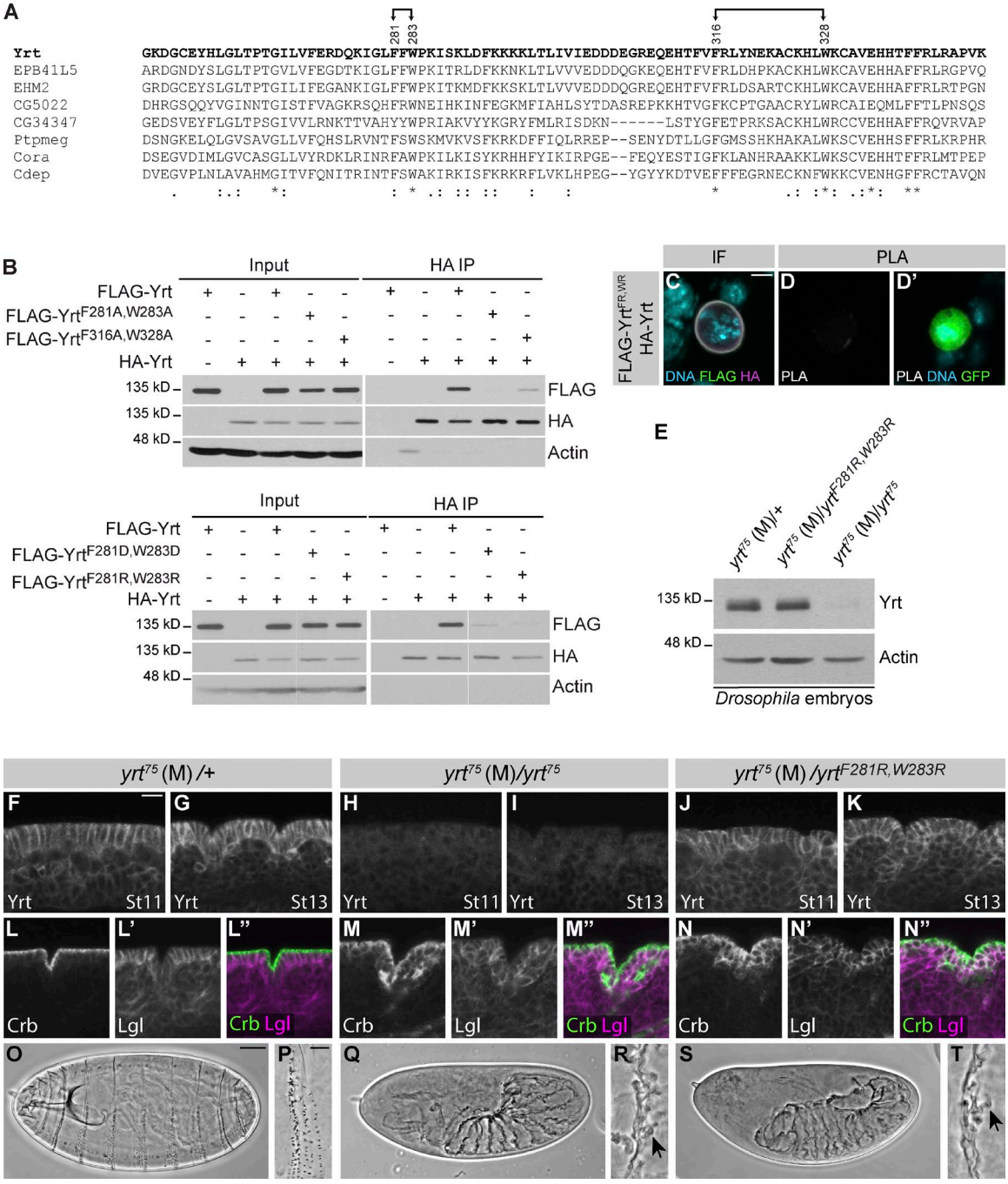

Figure 3. **The oligomerization of Yrt is essential for epithelial cell polarity. (A)** Alignment of the F3 lobe of the FERM domain of fly FERM-FA proteins, human EPB41L5, and human EHM2 (Larkin et al., 2007). Arrows indicate pairs of mutagenized amino acids. **(B)** S2 cells were transfected with the combination of constructs indicated above each lane and processed for immunoprecipitation with anti-HA antibodies. **(C)** Immunofluorescence performed on S2 cells cotransfected with HA-Yrt and FLAG-Yrt^{F281R,W283R} (referred to as FLAG-Yrt^{FR,WR}). **(D)** S2 cells cotransfected with GFP, HA-Yrt, and FLAG-Yrt^{F281R,W283R} were processed for PLA. Intrinsic GFP fluorescence was used to detect transfected cells. DNA was stained by using DAPI (C and D). Bar, 5 µm. **(E)** *yrt*^{75} germ line clone females (producing eggs devoid of maternal [M] Yrt; Chou and Perrimon, 1996; Laprise et al., 2006) were crossed with +/TM3-GFP, *yrt*^{F281R,W283R}/TM3-GFP, or *yrt*^{75}/TM3-GFP males. Stage 11–13 embryos were collected from each cross, and GFP-negative *yrt*^{75} (M)/+, *yrt*^{75} (M)/*yrt*^{75}, and *yrt*^{75} (M)/*yrt*^{F281R,W283R} were isolated. Harvested embryos were processed for Western blotting. **(F–N)** *yrt*^{75} (M)/+, *yrt*^{75} (M)/*yrt*^{75}, and *yrt*^{75} (M)/*yrt*^{F281R,W283R} embryos were fixed and stained for Yrt (F–K) or Crb and Lgl (L–N). Imaged embryos were at stage (St) 11 or 13. Bar, 10 µm. **(O–T)** Cuticle of *yrt*^{75} (M)/+ (O and P), *yrt*^{75} (M)/*yrt*^{75} (Q and R), and *yrt*^{75} (M)/*yrt*^{F281R,W283R} (S and T) embryos. Arrows point to convoluted cuticle. Bars: 60 µm (O, Q, and S); 15 µm (P, R, and T).

of Yrt expression, whereas maternal and zygotic *yrt*^{75} mutant embryos served as a negative control (Laprise et al., 2006). Yrt-F281R,W283R was expressed at a level similar to WT Yrt (Fig. 3 E) and was properly localized to the plasma membrane (Fig. 3, F–K) at embryonic stages where Yrt is required to maintain epithelial cell polarity (Laprise et al., 2009). Together, these results indicate that the Yrt^{F281R,W283R} mutant protein is suitable to study the physiological roles of Yrt oligomerization in vivo.

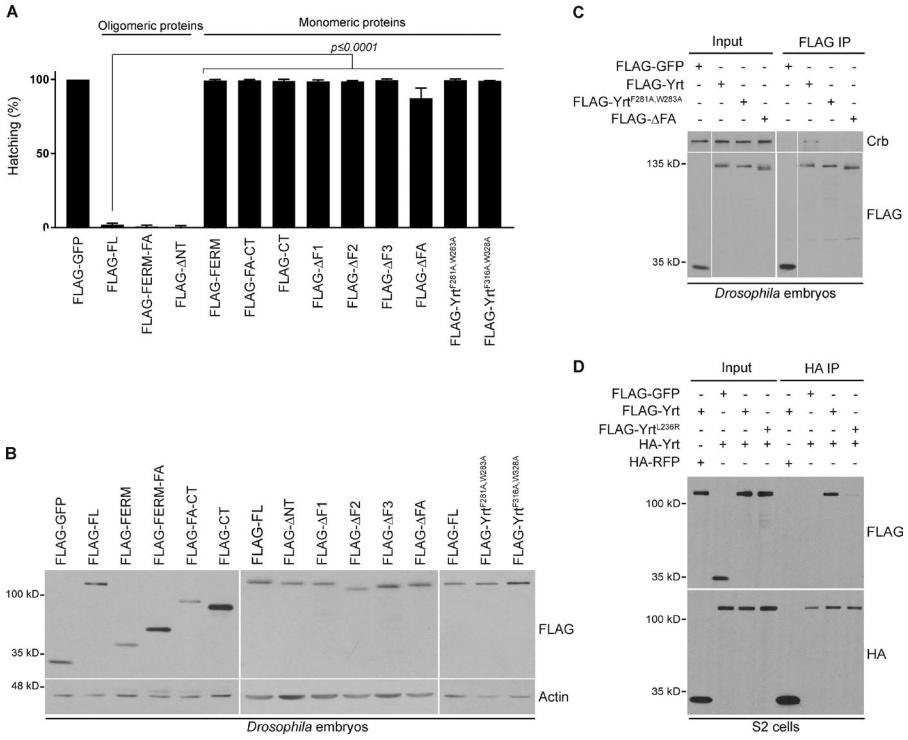

Figure 4. **The Yrt mutant proteins unable to oligomerize are inactive. (A)** Histogram showing the hatching percentage of control embryos expressing FLAG-GFP or of embryos expressing the indicated FLAG-tagged Yrt proteins (see Fig. 2, A and C). Error bars represent SD, and statistical significance was assessed by using Fisher's exact test (FLAG-GFP: $n = 390$; FLAG-FL: $n = 354$; FLAG–FERM-FA: $n = 234$; FLAG-ΔNT: $n = 381$; FLAG-FERM: $n = 254$; FLAG-FA-CT: $n = 254$; FLAG-CT: $n = 274$; FLAG-ΔF1: $n = 416$; FLAG-ΔF2: $n = 412$; FLAG-ΔF3: $n = 414$; FLAG-ΔFA: $n = 402$; FLAG-F281A, W283A: $n = 290$; and FLAG-F316A, W382A: $n = 322$). **(B)** Western blots showing the expression levels of the FLAG-tagged Yrt proteins used in the hatching assays. **(C)** Embryos expressing FLAG-GFP, FLAG-Yrt, FLAG-Yrt-^{F281A,W283A}, or FLAG-Yrt$^{\Delta FA}$ were homogenized, and an immunoprecipitation by using anti-FLAG antibodies was achieved. Western blotting was used to investigate the presence of endogenous Crb in the immunoprecipitate. **(D)** S2 cells expressing the indicated proteins were homogenized, and an immunoprecipitation by using anti-HA antibodies was performed. Proteins from immunocomplexes were detected by Western blotting.

Epithelial cells in *yrt* null embryos show polarity defects characterized by the ectopic localization of apical proteins such as Crumbs (Crb; Laprise et al., 2006, 2009) to the lateral membrane that is marked by lethal (2) giant larvae (Lgl; Fig. 3 L [control] and Fig. 3 M; Laprise et al., 2006, 2009). This polarity phenotype is accompanied by severe epithelial tissue defects, as shown by lack of head cuticle, and a large hole in the dorsal cuticle (Laprise et al., 2006; compare Fig. 3 O [control] with Fig. 3 Q). In addition, the ventral cuticle lacks denticle belts and is highly convoluted because of the enlarged apical, cuticle-secreting, membrane of epidermal cells (Laprise et al., 2006; compare Fig. 3 P with Fig. 3 R). Strikingly, embryos expressing Yrt^{F281R,W283R} displayed a ventral ectoderm phenotypically identical to embryos totally devoid of Yrt because they showed expansion of the Crb expression territory (Fig. 3 N). Moreover, Yrt^{F281R,W283R}-expressing embryos secreted a convoluted cuticle similar to *yrt* null embryos (Fig. 3, S and T; this phenotype is fully penetrant). These data demonstrate that the Yrt^{F281R,W283R} mutant protein is nonfunctional and strongly argue that Yrt needs to be in an oligomeric form to fulfill its function in epithelial cell polarity regulation.

To support the results obtained with the *yrt^{F281R,W283R}* allele, we used an overexpression-based structure–function analysis in *Drosophila* embryos. It was previously shown that overexpression of Yrt causes lethality, which results in part from exaggerated inhibition of proteins promoting apical membrane identity, including aPKC and Crb (Laprise et al., 2006; Gamblin et al., 2014). Expression of the FLAG-tagged Yrt truncations able to potently oligomerize also caused lethality (FLAG-FL, FLAG–FERM-FA, and FLAG-ΔNT; Fig. 2, A–D; and Fig. 4 A), and resulted in a similar cuticle phenotype (not depicted). In contrast, expression of the Yrt mutant proteins that show weak self-association or are unable to oligomerize had a limited impact on viability (FLAG-FERM, FLAG-FA-CT (C-terminal), FLAG-CT, FLAG-ΔF1, FLAG-ΔF2, FLAG-ΔF3, FLAG-ΔFA, FLAG-Yrt^{F281A,W283A}, FLAG-Yrt^{F316A,W328A}; Fig. 2, A–D; and Figs. 3 B and 4 A). Western blot experiments revealed that the lack of lethality does not result from reduced expression levels (Fig. 4 B), thus implying that mutant proteins incapable of oligomerizing are inactive. One important function of Yrt is to bind to Crb and to limit the activity of this apical determinant (Laprise et al., 2006). This raises the possibility that Yrt needs to oligomerize in order to associate with Crb. Accordingly, although FLAG-Yrt showed a clear association with endogenous Crb, the oligomerization-defective FLAG-Yrt^{F281A,W283A} and FLAG-Yrt$^{\Delta FA}$ proteins were unable to coprecipitate Crb (Fig. 4 C). A loss of function mutation that prevents binding of Mosaic Eyes (Moe; the zebra fish orthologue of Yrt; Hsu et al., 2006) to Crb was previously described (Ohata et al., 2011). We recreated this mutation in fly Yrt (Yrt^{L236R}) and showed that this mutant protein is unable to oligomerize (Fig. 4 D), thereby further supporting the notion that Yrt oligomerization promotes its binding to Crb. Together with the results obtained with the *yrt^{F281R,W283R}* allele, these data establish that the ability of Yrt to repress the Crb-containing apical machinery requires its multimerization.

aPKC dismantles the Yrt oligomer

It was previously established that phosphorylation of the FA domain by aPKC represses the function of Yrt (Gamblin et al., 2014). However, the molecular basis sustaining this inhibition remains undefined. We hypothesized that aPKC-mediated phosphorylation destabilizes the active Yrt oligomer. In accordance with this premise, knockdown of aPKC increased the amount of FLAG-Yrt that coprecipitated with HA-Yrt (Fig. 5 A). To obtain direct evidence that phosphorylation negatively impacts Yrt oligomerization, we used FLAG-Yrt^{5D} and FLAG-Yrt^{5A} in which the aPKC

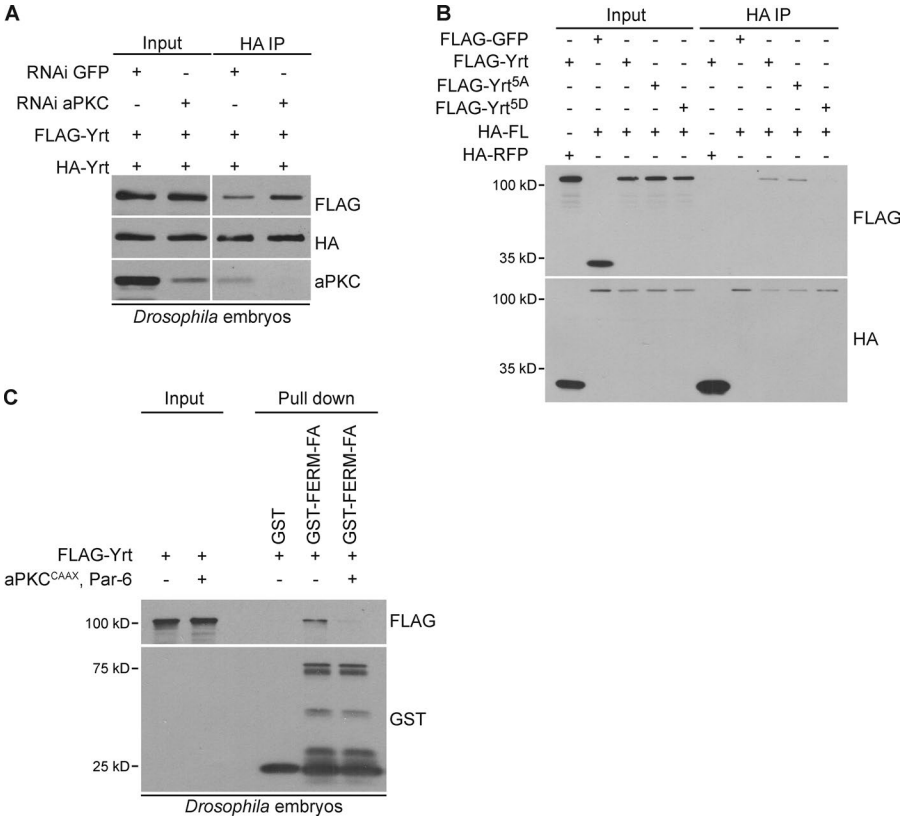

Figure 5. **The Yrt oligomer is destabilized by aPKC-dependent phosphorylation. (A)** FLAG-Yrt and HA-Yrt were coexpressed in aPKC-knockdown embryos (stage 11–13) or control embryos expressing an shRNA directed against GFP. An immunoprecipitation by using anti-HA antibodies was performed, and Western blotting revealed the amount of FLAG-Yrt, HA-Yrt, and aPKC in the immunocomplexes. **(B)** S2 cells expressing the indicated proteins were homogenized, and an HA immunoprecipitation was performed. Immunoprecipitated proteins were detected by Western blotting. **(C)** GST–FERM-FA was used to pull down FLAG-Yrt expressed in a WT background or in embryos expressing aPKC^{CAAX} together with Par-6 (stage 15–17 embryos). GST was used as a negative pulldown control.

phosphorylation sites within the FA domain were mutagenized to phosphomimetic D residues or to nonphosphorylatable A residues, respectively (Gamblin et al., 2014). The phosphomimetic FLAG-Yrt^{5D} showed much-reduced binding to HA-Yrt in S2 cells compared with WT FLAG-Yrt or with the nonphosphorylatable FLAG-Yrt^{5A} (Fig. 5 B). As a complement to the latter experiment, we used the truncated GST–FERM-FA protein (Fig. 1 B) to pull down FLAG-Yrt expressed in a WT background or in embryos expressing activated aPKC (aPKC^{CAAX}) together with its regulator Par-6 (Sotillos et al., 2004; David et al., 2010; Tepass, 2012). Expression of aPKC^{CAAX} and Par-6 results in a massive phosphorylation of Yrt (Gamblin et al., 2014) and strongly reduced the amount of FLAG-Yrt pulled down by GST–FERM-FA (Fig. 5 C). Collectively, these results establish that aPKC-dependent phosphorylation prevents Yrt oligomerization. This function may not be exclusive to aPKC because it was recently demonstrated that the kinase Pak1 acts redundantly with aPKC to maintain apical membrane identity (Aguilar-Aragon et al., 2018). Our findings may help explain how phosphorylation of the FA domain represses the function of other FERM-FA proteins (Baines, 2006; Nakajima and Tanoue, 2012).

Overall, our study demonstrates that the ability of Yrt to bind to Crb and to maintain epithelial cell polarity depends strictly on its oligomerization via the FERM and FA domains. We thus assigned a novel molecular function to the FA domain (Baines, 2006). We also discovered that aPKC-dependent phosphorylation dismantles the Yrt oligomer, thus elucidating the molecular basis whereby aPKC inhibits Yrt function (Gamblin et al., 2014). This observation could apply to other aPKC substrates such as Bazooka (Baz)/PAR-3 and Lgl that oligomerize (Strand et al., 1994; Benton and St Johnston, 2003). Similar to Yrt, these proteins are displaced from the apical membrane after their phosphorylation by aPKC, a critical step in establishing polarity (Hutterer et al., 2004; Morais-de-Sá et al., 2010; Walther and Pichaud, 2010; Gamblin et al., 2014). The phosphorylation of aPKC substrates neutralizes the positive charge of basic and hydrophobic motifs, thereby precluding binding of these proteins to phospholipids (Bailey and Prehoda, 2015; Dong et al., 2015). As aPKC alters the cortical localization of Yrt (Gamblin et al., 2014), a similar mechanism could control the association of Yrt to the membrane. Further analysis of how aPKC regulates the function of Yrt and its other substrates is fundamental to understanding the mechanisms organizing cell polarity and to deciphering the etiology of human diseases (Coradini et al., 2011; Tepass, 2012).

Materials and methods

Molecular biology

By using the In-Fusion cloning kit (Takara Bio Inc.) according to the manufacturer's instructions, DNA fragments were subcloned in pGEX-6p-2, pUASTattB (provided by K. Basler, University of Zurich, Zurich, Switzerland), pcDNA3, or pcDNA3.1. All clones were fully sequenced. Protein domains in Yrt were predicted with InterPro (http://www.ebi.ac.uk/interpro/), and the sequence of Yrt was also analyzed with PSIPRED (Buchan et al., 2013) to ensure that secondary structures were maintained in truncated proteins.

Transgenic fly lines

BestGene Inc. performed the injection in *Drosophila* embryos carrying an attP docking site (Groth et al., 2004). Specifically,

we used stocks 24485 and 24481 for FLAG-tagged constructs, or 24482 and 24749 for HA-tagged constructs (Bloomington Drosophila Stock Center [BDSC]; these lines were produced by K. Basler's group). The following transgenic lines were produced: P{UAS-3×FLAG-*yrt*.FL}, P{UAS-2×HA-*yrt*.FL}, P{UAS-3×FLAG-*yrt*.FERM}, P{UAS-3×FLAG-*yrt*.FERM-FA}, P{UAS-3×FLAG-*yrt*.FA-CT}, P{UAS-3×FLAG-*yrt*.CT}, P{UAS-3×FLAG-*yrt*.ΔNT}, P{UAS-3×FLAG-*yrt*.ΔF1}, P{UAS-3×FLAG-*yrt*.ΔF2}, P{UAS-3×FLAG-*yrt*.ΔF3}, P{UAS-3×FLAG-*yrt*.ΔFA}, P{UAS-3×FLAG-*yrt*.F281A,W283A}, P{UAS-3×FLAG-*yrt*.F316A,W328A}, P{UAS-3×FLAG-*yrt*.L236R}, P{UAS-3×FLAG-GFP10}, and P{UAS-2×HA-RFP}.

CRISPR/Cas9-mediated mutagenesis

Mutation of the *yrt* locus was performed by using the Scarless gene editing system (Gratz et al., 2015; http://flycrispr.molbio.wisc.edu/scarless). The guide RNA (5′-CTGGCCCAAGATCAGTAAGCTGG-3′) was cloned in pU6-BbsI-gRNA (Drosophila Genomics Resource Center; produced by the group of K. O'Connor-Giles, University of Winsconsin-Madison, Madison, WI), and validated in S2 cells by using the Guide-it mutation detection kit (Takara Bio Inc.) according to the manufacturer's instructions. The donor DNA was cloned in pHD-ScarlessDsRed (Drosophila Genomics Resource Center; K. O'Connor-Giles). The donor DNA extended 1 kb on each side of the cleavage site and contained the mutations of interest. Specifically, the sequence TTCTTCTGG (nucleotides 2,340–2,348 of the *yrt* gene) was mutagenized to CGTTTCCGT in order to change F281 and W283 to R residues. In addition, nucleotide 2,366 was mutagenized to generate a silent mutation in the protospacer adjacent motif (G to T mutation). Plasmid injection was performed at BestGene Inc. in y[1] sc[1] v[1]; P{nos-Cas9}attP40/CyO embryos (Ren et al., 2013). Flies that successfully integrated the donor DNA in the *yrt* locus were crossed with w[1118]; CyO, P{Tub-PBac\T}2/wg[Sp-1] flies to remove the DsRed cassette. Finally, mutations of interest at the *yrt* locus were confirmed by sequencing, which extended beyond the homology arms of the donor DNA.

Drosophila genetics

Germ line clone females (null allele yrt^{75}) were produced to remove maternal Yrt as previously described (Chou and Perrimon, 1996; Laprise et al., 2006) and were crossed to males of the following genotypes: (1) +/TM3, P{w[+mC]=GAL4-twi.G}2.3, P{UAS-2×EGFP}AH2.3, Sb[1] Ser[1]; (2) $yrt^{F281R,W283R}$/TM3, P{w[+mC]=GAL4-twi.G}2.3, P{UAS-2×EGFP}AH2.3, Sb[1] Ser[1]; or (3) yrt^{75}/TM3, P{w[+mC]=GAL4-twi.G}2.3, P{UAS-2×EGFP}AH2.3, Sb[1] Ser[1]. GFP fluorescence was used to identify and remove embryos carrying the balancer chromosome. Expression of exogenous proteins was induced in fly embryos by crossing respective UAS lines with the da-GAL4 driver line (Wodarz et al., 1995) at 25°C. The maternal driver line matαtub67;15 (provided by D. St-Johnston, University of Cambridge, Cambridge, England, UK) was crossed to y[1] sc[*] v[1]; P{y[+t7.7] v[+t1.8]=TRiP.HMS01320}attP2 flies (BDSC stock 34332) at 25°C to knockdown aPKC. An shRNA targeting EGFP was used as control (P{VALIUM20-EGFP.shRNA.4}attP2; BDSC stock 41553).

Cell culture and transfection

S2 cells were grown at RT in Schneider's medium (Wisent Inc.) supplemented with 10% heat-inactivated FBS (Wisent Inc.), 50 U/ml penicillin, and 50 µg/ml streptomycin (Thermo Fisher Scientific). When they reached 60% of confluence, S2 cells were transfected by calcium phosphate precipitation with pAct5c-Gal4 together with selected pUASTattB-based plasmids. In preparation to immunofluorescence or PLA, S2 cells were seeded on glass coverslips coated with a solution of 0.5 mg/ml of Concanavalin A (Sigma-Aldrich) and incubated for 45 min at RT for proper adhesion. MDCK II cells were grown in DMEM supplemented with 10% FBS, 2 mM glutamine, 10 mM Hepes, 50 U/ml penicillin, 50 µg/ml streptomycin, and 1× MEM nonessential amino acids (Thermo Fisher Scientific). Cells were maintained at 37°C under a humidified atmosphere containing 5% of CO_2. Cells were transfected at a density of 70% by using Lipofectamine 2000 according to manufacturer's instructions (Thermo Fisher Scientific). For immunostainings and PLA experiments, MDCK II cells were grown on glass coverslips.

Immunofluorescence microscopy

Drosophila embryos were dechorionated, heat fixed, and processed for immunofluorescence as previously described (Gamblin et al., 2014). Embryos were incubated with primary antibodies, which were diluted in normal goat serum–Triton X-100 (0.3% Triton X-100 and 2% normal goat serum in PBS), for 16 h at 4°C. Primary antibodies used were rat anti-Crb (1:500; Pellikka et al., 2002), guinea pig anti-Yrt (1:250; Laprise et al., 2006), and Lgl (1:100, D300; Santa Cruz Biotechnology). Embryos were then washed three times with PBS containing 0.3% Triton X-100, and incubated for 1 h at RT with secondary antibodies diluted 1:400 in PBS containing 0.3% Triton X-100. The following secondary antibodies were used: Cy3 anti-guinea pig, Cy3 anti-rabbit, and Alexa Fluor 488 anti-rat (Jackson ImmunoResearch Laboratories).

MDCK II and S2 cells were fixed, permeabilized, saturated, incubated with primary and secondary antibodies, and stained with DAPI as previously described (Loie et al., 2015). Primary antibodies used were mouse anti-HA (1:1,000, clone 16B12; BioLegend), rabbit anti-GFP (1:250; Thermo Fisher Scientific), and rabbit anti-FLAG (1:250; Sigma-Aldrich). Secondary antibodies used were anti-mouse Cy3 and anti-rabbit Alexa Fluor 488 (1:400; Jackson ImmunoResearch Laboratories). Embryos and cells were mounted in Vectashield (Vector Laboratories). All images were acquired by using a confocal microscope (FV1000; Olympus) by using a 40× Apochromat lens or a PLAPON 60× lens with a numerical aperture of 0.90 and 1.42, respectively. Images were uniformly processed by using ImageJ (National Institutes of Health), Olympus FV1000 viewer (v.4.2b), or Photoshop (CC 2017; Adobe).

PLA

Cells were fixed and processed as described for immunofluorescence (see previous section). Cells were incubated for 16 h at 4°C in a wet chamber with mouse anti-HA (clone 16B12; BioLegend) and rabbit anti-FLAG (Sigma-Aldrich), both diluted 1:250. The PLA kit (Duolink In Situ Red Starter Kit Mouse/Rabbit; Sigma-Aldrich) was used according to the manufacturer's instructions.

The slides were mounted with mounting medium containing DAPI (provided with the PLA kit).

Immunoprecipitation

PBS-washed S2 cells or dechorionated embryos were homogenized in ice-cold lysis buffer (HA immunoprecipitations: 50 mM Tris-HCl, pH 7.4, 150 mM NaCl, 1 mM EDTA, 0.75% NP-40, 0.1 mM sodium orthovanadate, 0.1 mM phenylmethylsulfonyl fluoride, 1 mM NaF, 10 µg/ml aprotinin, 10 µg/ml leupeptin, and 0.7 µg/ml pepstatin; FLAG immunoprecipitations: 50 mM Tris-HCl, pH 7.5, 100 mM NaCl, 5 mM EDTA, pH 8, 5% glycerol, 1% Triton X-100, 40 mM β-glycerophosphate, 0.1 mM sodium orthovanadate, 0.1 mM phenylmethylsulfonyl fluoride, 50 mM NaF, 10 µg/ml aprotinin, 10 µg/ml leupeptin, and 0.7 µg/ml pepstatin). Cellular debris was then removed by centrifugation (17,000 *g* for 10 min at 4°C), and embryo or S2 cell lysates containing 500 µg to 1.5 mg of total proteins were precleared for 90 min under agitation with 15 µl of a suspension of protein G Sepharose beads (50% in lysis buffer; GE Healthcare). Supernatants were then incubated with 0.5 µg of the anti-HA antibody (clone 16B12; BioLegend) or with 20 µl of anti-FLAG-agarose (A2220; Sigma-Aldrich) for 1.5 h at 4°C under agitation. HA immunocomplexes were further incubated (1 h at 4°C) with 15 µl protein G Sepharose beads. Beads were harvested by centrifugation and washed five times with lysis buffer. Proteins were eluted with Laemmli buffer.

Protein purification

pGEX-6p-2 plasmids were transformed in BL21(DE3) cells, which were grown in Terrific Broth (BioBasic) containing 0.2% glucose. Addition of 0.1 mM IPTG to bacterial cultures (OD of 0.6 at 600 nm) for 16 h at 16°C induced protein expression. Proteins were purified by using the GST tag according to the method described by Frangioni and Neel (1993) by using 1.5% sarcosyl and 2.5% Triton X-100. GST or GST–FERM-FA was eluted with 20 mM glutathione, whereas GST-FL-His was eluted with the PreScission protease (Maity et al., 2013), which removed the GST tag. The FL-His protein was further purified by using TALON Metal Affinity Resin (Takara Bio Inc.) as previously described (Maity et al., 2013). All proteins were twice dialyzed for 1 h in 20 mM Tris, pH 7.5, 150 mM NaCl, 10% glycerol, and 1 mM DTT. Finally, cOmplete EDTA-free protease inhibitor cocktail (Sigma-Aldrich) was added to purified protein solutions.

GST pulldown

Embryos were homogenized in ice-cold lysis buffer (50 mM Tris-HCl, pH 7.4, 150 mM NaCl, 1 mM EDTA, 1% Triton X-100, 0.1 mM sodium orthovanadate, 0.1 mM phenylmethylsulfonyl fluoride, 1 mM NaF, 10 µg/ml aprotinin, 10 µg/ml leupeptin, 0.7 µg/ml pepstatin, 1 mM sodium pyrophosphate, and 1 mM β glycerophosphate) and processed as previously described (Gamblin et al., 2014). Then, 0.5 µg GST or GST-fusion proteins was added to embryo lysates (400 µg total proteins) or to 0.5 µg purified YrtFL-His. Protein mixes were incubated for 1 h at 4°C before addition of 40 µl of Glutathione-Sepharose beads (GE Healthcare; 50% suspension in lysis buffer), and samples were further incubated under agitation for 1 h at 4°C. Beads were washed five times with ice-cold lysis buffer. For the pull-down experiments performed on embryo lysates, an additional wash was performed with lysis buffer devoid of phosphatase inhibitors. Then, pulled-down proteins were dephosphorylated with the λ phosphatase (New England Biolabs) according to the manufacturer's instructions. Finally, proteins were eluted with Laemmli buffer.

Western blotting

Sample homogenization and Western blotting were performed as previously described (Laprise et al., 2002; Gamblin et al., 2014). Primary antibodies used were guinea pig anti-Yrt (1:5,000; Laprise et al., 2006); rabbit anti-aPKC (1:2,000, C20; Santa Cruz Biotechnology), mouse anti-FLAG (1:2,500, clone M2; Sigma-Aldrich), mouse anti-HA (1:2,000, clone 16B12; BioLegend), mouse anti-His (1:2,000; Takara Bio Inc.), mouse anti-actin (1:10,000, clone C4; Chemicon), and rabbit anti-GST (1:8,000; provided by J.-Y. Masson, Université Laval, Québec City, Canada). HRP-conjugated secondary antibodies were used at a 1:2,000 dilution. The secondary antibody mouse TrueBlot ULTRA (1:1,000; Rockland) was used for blotting of membranes on which immunoprecipitation experiments were transferred.

Determination of hatching percentages

Freshly laid embryos were placed on an apple plate and incubated for 72 h at 25°C. Larvae and dead embryos were then scored, and the hatching percentage was determined by the ratio of living larvae on the number of larvae plus dead embryos × 100. The experiments were performed in triplicate for a total of at least 234 embryos for each genotype.

Sequence alignment

Sequence alignment was performed by using ClustalW (Larkin et al., 2007).

Cuticle preparation

Embryos were dechorionated (Gamblin et al., 2014) and incubated at 85°C for 16 h in a mixture of Hoyer's mounting media and lactic acid (1:1).

Statistical analysis

Data were presented as means ± SD. Statistical analyses were performed by using Prism 7 (GraphPad Software). Differences between individual groups were analyzed by using Fisher's exact test (95% confidence intervals, two-tailed). P values <0.05 were considered statistically significant.

Online supplemental material

Fig. S1 shows that oligomerization is not required for the localization of Yrt to the membrane.

Acknowledgments

We thank K. O'Connor-Giles, N. Perrimon, D. St Johnston, T. Harris, M. Bouvier, J.-Y. Masson, the BDSC, Addgene, the Drosophila Genomics Resource Center, and the Developmental Studies Hybridoma Bank for reagents. FlyBase was an important resource for our study.

This study was supported by an operating grant from the Canadian Institutes of Health Research to P. Laprise (MOP-142236).

The authors declare no competing financial interests.

Author contributions: P. Laprise and C. Gamblin conceived the project, and C. Gamblin performed most experiments. P. Laprise, C. Gamblin, F. Parent-Prévost, and C. Biehler interpreted the results. F. Parent-Prévost, K. Jacquet, C. Biehler, and A. Jetté also performed experiments, prepared reagents, and contributed to data analysis. P. Laprise wrote the manuscript with the help of C. Gamblin and K. Jacquet. Finally, P. Laprise, C. Gamblin, K. Jacquet, and F. Parent-Prévost assembled the figures. All authors read and approved the final manuscript.

Submitted: 16 March 2018
Revised: 18 July 2018
Accepted: 24 July 2018

References

Aguilar-Aragon, M., A. Elbediwy, V. Foglizzo, G.C. Fletcher, V.S.W. Li, and B.J. Thompson. 2018. Pak1 kinase maintains apical membrane identity in epithelia. *Cell Reports*. 22:1639–1646. https://doi.org/10.1016/j.celrep.2018.01.060

Bailey, M.J., and K.E. Prehoda. 2015. Establishment of Par-polarized cortical domains via phosphoregulated membrane motifs. *Dev. Cell*. 35:199–210. https://doi.org/10.1016/j.devcel.2015.09.016

Baines, A.J. 2006. A FERM-adjacent (FA) region defines a subset of the 4.1 superfamily and is a potential regulator of FERM domain function. *BMC Genomics*. 7:85. https://doi.org/10.1186/1471-2164-7-85

Baines, A.J., H.C. Lu, and P.M. Bennett. 2014. The Protein 4.1 family: Hub proteins in animals for organizing membrane proteins. *Biochim. Biophys. Acta*. 1838:605–619. https://doi.org/10.1016/j.bbamem.2013.05.030

Benton, R., and D. St Johnston. 2003. A conserved oligomerization domain in drosophila Bazooka/PAR-3 is important for apical localization and epithelial polarity. *Curr. Biol.* 13:1330–1334. https://doi.org/10.1016/S0960-9822(03)00508-6

Buchan, D.W.A., F. Minneci, T.C.O. Nugent, K. Bryson, and D.T. Jones. 2013. Scalable web services for the PSIPRED Protein Analysis Workbench. *Nucleic Acids Res.* 41(W1):W340–W348.

Chou, T.B., and N. Perrimon. 1996. The autosomal FLP-DFS technique for generating germline mosaics in Drosophila melanogaster. *Genetics*. 144:1673–1679.

Coradini, D., C. Casarsa, and S. Oriana. 2011. Epithelial cell polarity and tumorigenesis: New perspectives for cancer detection and treatment. *Acta Pharmacol. Sin.* 32:552–564. https://doi.org/10.1038/aps.2011.20

David, D.J., A. Tishkina, and T.J. Harris. 2010. The PAR complex regulates pulsed actomyosin contractions during amnioserosa apical constriction in Drosophila. *Development*. 137:1645–1655. https://doi.org/10.1242/dev.044107

Dong, W., X. Zhang, W. Liu, Y.J. Chen, J. Huang, E. Austin, A.M. Celotto, W.Z. Jiang, M.J. Palladino, Y. Jiang, et al. 2015. A conserved polybasic domain mediates plasma membrane targeting of Lgl and its regulation by hypoxia. *J. Cell Biol.* 211:273–286. https://doi.org/10.1083/jcb.201503067

Frangioni, J.V., and B.G. Neel. 1993. Solubilization and purification of enzymatically active glutathione S-transferase (pGEX) fusion proteins. *Anal. Biochem.* 210:179–187. https://doi.org/10.1006/abio.1993.1170

Gamblin, C.L., E.J. Hardy, F.J. Chartier, N. Bisson, and P. Laprise. 2014. A bidirectional antagonism between aPKC and Yurt regulates epithelial cell polarity. *J. Cell Biol.* 204:487–495. https://doi.org/10.1083/jcb.201308032

Gosens, I., A. Sessa, A.I. den Hollander, S.J. Letteboer, V. Belloni, M.L. Arends, A. Le Bivic, F.P. Cremers, V. Broccoli, and R. Roepman. 2007. FERM protein EPB41L5 is a novel member of the mammalian CRB-MPP5 polarity complex. *Exp. Cell Res.* 313:3959–3970. https://doi.org/10.1016/j.yexcr.2007.08.025

Gratz, S.J., C.D. Rubinstein, M.M. Harrison, J. Wildonger, and K.M. O'Connor-Giles. 2015. CRISPR-Cas9 genome editing in Drosophila. *Curr. Protoc. Mol. Biol.* 111:1–20.

Groth, A.C., M. Fish, R. Nusse, and M.P. Calos. 2004. Construction of transgenic Drosophila by using the site-specific integrase from phage phiC31. *Genetics*. 166:1775–1782. https://doi.org/10.1534/genetics.166.4.1775

Hamada, K., T. Shimizu, T. Matsui, S. Tsukita, and T. Hakoshima. 2000. Structural basis of the membrane-targeting and unmasking mechanisms of the radixin FERM domain. *EMBO J.* 19:4449–4462. https://doi.org/10.1093/emboj/19.17.4449

Hsu, Y.C., J.J. Willoughby, A.K. Christensen, and A.M. Jensen. 2006. Mosaic Eyes is a novel component of the Crumbs complex and negatively regulates photoreceptor apical size. *Development*. 133:4849–4859. https://doi.org/10.1242/dev.02685

Hutterer, A., J. Betschinger, M. Petronczki, and J.A. Knoblich. 2004. Sequential roles of Cdc42, Par-6, aPKC, and Lgl in the establishment of epithelial polarity during Drosophila embryogenesis. *Dev. Cell*. 6:845–854. https://doi.org/10.1016/j.devcel.2004.05.003

Laprise, P., P. Chailler, M. Houde, J.F. Beaulieu, M.J. Boucher, and N. Rivard. 2002. Phosphatidylinositol 3-kinase controls human intestinal epithelial cell differentiation by promoting adherens junction assembly and p38 MAPK activation. *J. Biol. Chem.* 277:8226–8234. https://doi.org/10.1074/jbc.M110235200

Laprise, P., S. Beronja, N.F. Silva-Gagliardi, M. Pellikka, A.M. Jensen, C.J. McGlade, and U. Tepass. 2006. The FERM protein Yurt is a negative regulatory component of the Crumbs complex that controls epithelial polarity and apical membrane size. *Dev. Cell*. 11:363–374. https://doi.org/10.1016/j.devcel.2006.06.001

Laprise, P., K.M. Lau, K.P. Harris, N.F. Silva-Gagliardi, S.M. Paul, S. Beronja, G.J. Beitel, C.J. McGlade, and U. Tepass. 2009. Yurt, Coracle, Neurexin IV and the Na(+),K(+)-ATPase form a novel group of epithelial polarity proteins. *Nature*. 459:1141–1145. https://doi.org/10.1038/nature08067

Larkin, M.A., G. Blackshields, N.P. Brown, R. Chenna, P.A. McGettigan, H. McWilliam, F. Valentin, I.M. Wallace, A. Wilm, R. Lopez, et al. 2007. Clustal W and Clustal X version 2.0. *Bioinformatics*. 23:2947–2948. https://doi.org/10.1093/bioinformatics/btm404

Loie, E., L.E. Charrier, K. Sollier, J.Y. Masson, and P. Laprise. 2015. CRB3A controls the morphology and cohesion of cancer cells through Ehm2/p114RhoGEF-dependent signaling. *Mol. Cell. Biol.* 35:3423–3435. https://doi.org/10.1128/MCB.00673-15

Maity, R., J. Pauty, J. Krietsch, R. Buisson, M.M. Genois, and J.Y. Masson. 2013. GST-His purification: A two-step affinity purification protocol yielding full-length purified proteins. *J. Vis. Exp.* Oct 29:e50320.

Morais-de-Sá, E., V. Mirouse, and D. St Johnston. 2010. aPKC phosphorylation of Bazooka defines the apical/lateral border in Drosophila epithelial cells. *Cell*. 141:509–523. https://doi.org/10.1016/j.cell.2010.02.040

Nakajima, H., and T. Tanoue. 2012. The circumferential actomyosin belt in epithelial cells is regulated by the Lulu2-p114RhoGEF system. *Small GTPases*. 3:91–96. https://doi.org/10.4161/sgtp.19112

Ohata, S., R. Aoki, S. Kinoshita, M. Yamaguchi, S. Tsuruoka-Kinoshita, H. Tanaka, H. Wada, S. Watabe, T. Tsuboi, I. Masai, and H. Okamoto. 2011. Dual roles of Notch in regulation of apically restricted mitosis and apicobasal polarity of neuroepithelial cells. *Neuron*. 69:215–230. https://doi.org/10.1016/j.neuron.2010.12.026

Pearson, M.A., D. Reczek, A. Bretscher, and P.A. Karplus. 2000. Structure of the ERM protein moesin reveals the FERM domain fold masked by an extended actin binding tail domain. *Cell*. 101:259–270. https://doi.org/10.1016/S0092-8674(00)80836-3

Pellikka, M., G. Tanentzapf, M. Pinto, C. Smith, C.J. McGlade, D.F. Ready, and U. Tepass. 2002. Crumbs, the Drosophila homologue of human CRB1/RP12, is essential for photoreceptor morphogenesis. *Nature*. 416:143–149. https://doi.org/10.1038/nature721

Ren, X., J. Sun, B.E. Housden, Y. Hu, C. Roesel, S. Lin, L.P. Liu, Z. Yang, D. Mao, L. Sun, et al. 2013. Optimized gene editing technology for Drosophila melanogaster using germ line-specific Cas9. *Proc. Natl. Acad. Sci. USA*. 110:19012–19017. https://doi.org/10.1073/pnas.1318481110

Söderberg, O., M. Gullberg, M. Jarvius, K. Ridderstråle, K.J. Leuchowius, J. Jarvius, K. Wester, P. Hydbring, F. Bahram, L.G. Larsson, and U. Landegren. 2006. Direct observation of individual endogenous protein complexes in situ by proximity ligation. *Nat. Methods*. 3:995–1000. https://doi.org/10.1038/nmeth947

Sotillos, S., M.T. Díaz-Meco, E. Caminero, J. Moscat, and S. Campuzano. 2004. DaPKC-dependent phosphorylation of Crumbs is required for epithelial cell polarity in Drosophila. *J. Cell Biol.* 166:549–557. https://doi.org/10.1083/jcb.200311031

Strand, D., R. Jakobs, G. Merdes, B. Neumann, A. Kalmes, H.W. Heid, I. Husmann, and B.M. Mechler. 1994. The Drosophila lethal(2)giant larvae tumor suppressor protein forms homo-oligomers and is associated with

nonmuscle myosin II heavy chain. *J. Cell Biol.* 127:1361–1373. https://doi.org/10.1083/jcb.127.5.1361

Tepass, U. 2009. FERM proteins in animal morphogenesis. *Curr. Opin. Genet. Dev.* 19:357–367. https://doi.org/10.1016/j.gde.2009.05.006

Tepass, U. 2012. The apical polarity protein network in Drosophila epithelial cells: Regulation of polarity, junctions, morphogenesis, cell growth, and survival. *Annu. Rev. Cell Dev. Biol.* 28:655–685. https://doi.org/10.1146/annurev-cellbio-092910-154033

Walther, R.F., and F. Pichaud. 2010. Crumbs/DaPKC-dependent apical exclusion of Bazooka promotes photoreceptor polarity remodeling. *Curr. Biol.* 20:1065–1074. https://doi.org/10.1016/j.cub.2010.04.049

Wodarz, A., U. Hinz, M. Engelbert, and E. Knust. 1995. Expression of crumbs confers apical character on plasma membrane domains of ectodermal epithelia of Drosophila. *Cell.* 82:67–76. https://doi.org/10.1016/0092-8674(95)90053-5